ARMY RESEARCH LABORATORY

Modeling Dynamic Behavior and Texture Evolution in Pure Tantalum (Ta)

by S. E. Schoenfeld, S. Ahzi,
and K. S. Vecchio

ARL-TR-1530 October 1997

The findings in this report are not to be construed as an official Department of the Army position unless so designated by other authorized documents.

Citation of manufacturer's or trade names does not constitute an official endorsement or approval of the use thereof.

Destroy this report when it is no longer needed. Do not return it to the originator.

Army Research Laboratory
Aberdeen Proving Ground, MD 21005-5066

ARL-TR-1530 **October 1997**

Modeling Dynamic Behavior and Texture Evolution in Pure Tantalum (Ta)

S. E. Schoenfeld
Weapons and Materials Research Directorate, ARL

S. Ahzi
Department of Mechanical Engineering, Clemson University

K. S. Vecchio
Department of Applied Mechanics and Engineering Science
University of California, San Diego

Abstract

In order to model high-strain-rate deformation and texture evolution in commercially pure tantalum (Ta), a description for the thermal-elastic-viscoplastic behavior of Ta single crystals is considered along with an associated polycrystal averaging scheme. The description incorporates a temperature-dependent model for pencil glide on the planes of maximum-resolved shear stress. Calculated stress-strain data and texture evolution for this model are compared to those of a restricted-glide model and to experimental data.

Acknowledgments

K. Vecchio acknowledges the support of the U. S. Army Research Office (ARO) through a University Research Initiative (URI) at the University of California, San Diego (UCSD). S. Ahzi would like to acknowledge support from the Mechanical Engineering Department, Clemson University. S. Schoenfeld would like to acknowledge the support of the U. S. Army Research Laboratory, Weapons and Materials Research Directorate (WMRD). Helpful discussions with Dr. G. T. Gray III and J. R. K. Garrett are gratefully acknowledged; the material was also supplied by Dr. Gray. The assistance of Mr. Jon Isaacs in conducting the high-strain-rate experiments is appreciated.

INTENTIONALLY LEFT BLANK

Table of Contents

INTENTIONALLY LEFT BLANK

List of Figures

INTENTIONALLY LEFT BLANK

List of Tables

INTENTIONALLY LEFT BLANK

1. Introduction

Tantalum (Ta) is a high-density body-centered cubic (bcc) metal that is highly ductile over a wide range of temperatures and strain rates. The high density of Ta makes it an attractive candidate for penetration applications while its high ductility translates to high formability under the broad range of processing environments that must be tolerated by an explosively deformed liner. Wrought Ta is most commonly available in the form of rolled plate, which must undergo deep drawing to form the initial liner. Prior to the penetration event, the initial liner is either deep drawn or fully collapsed at high strain rate to form an elongated cup or rod in the reverse direction of initial drawing.

The drawability of sheet material has long been recognized to depend on material flow coming from the width and not the thickness of the rolled sheet (Backofen 1972). For bcc steels, this flow property has been shown to depend on the alignment of {111} planes with the rolling plane of the sheet (Lankford, Snyder, and Bauscher 1950). Such crystallographic texture considerations are also expected to influence the deep-drawing rolled Ta sheet. With this in mind, Clark et al. (1991) showed the effects of forging and rolling conditions on through-thickness texture gradients in Ta liner material. Their goal was to produce Ta sheet with a homogeneous through-thickness microstructure.

In order to develop predictive capabilities for the thermomechanical processing of Ta, a temperature- and rate-dependent model is presented for finite-strain deformation by $< 111 >$ crystallographic slip that is not restricted to particular crystallographic planes (pencil glide). The model is based on the Asaro and Needleman (1985) elastic-viscoplastic formulation for rate-dependent crystallographic slip in polycrystalline aggregates. In this model, the stress state in each particular grain is uniquely determined from the elastically deforming crystal lattice. This stress state is then used to determine crystallographic planes via a maximum-resolved shear-stress criteria originally outlined by Becker (1995). The determination of the slip planes is conducted throughout the entire deformation process (i.e., evaluated at each time step during the calculation). This model allows for the wavy glide nature of $< 111 > \{110\}$ and $< 111 > \{121\}$ crystallographic slip in bcc metals. It should also be noted that although only homogeneous deformations are considered at present, this model may be particularly well suited for implementation within a finite-element framework to simulate the entire thermomechanical process. Since the maximum-resolved shear-stress criteria determines the proper slip planes as the computation proceeds, there is only a single-plane normal calculated per slip direction, and the orientation of this normal is allowed to evolve during the deformation. This approach reduces the number of slip systems typically required to model bcc restricted glide to only the four pencil-glide directions and their associated slip-plane normals. The temperature dependence of the slip rate is incorporated by the exponential temperature dependence recently proposed by Lee et al. (1997). As such, the model can account for thermal softening due to adiabatic heating that accompanies high-rate deformation during explosive forming. The stress-strain behavior and associated texture evolution predicted by the model are compared with experimental results obtained at high strain rates.

Notation used in this paper is based on the following conventions. Scalars are denoted by

mathematical italics or calligraphics (A, a, α, $\mathcal{X}$), vectors by lowercase boldface ($\mathbf{a}$), second-order tensors by uppercase boldface ($\mathbf{A}$), and fourth-order tensors by calligraphic uppercase boldface ($\boldsymbol{\mathcal{K}}$). The boldface Greek letters designate second-order tensors. The summation convention is used for Latin indices. Superscripts pertaining to slip systems are written in Greek letters; summation over these are indicated explicitly. Single dots and double dots are used to indicate the following products, respectively:

$$\mathbf{F} \cdot \mathbf{m} \rightleftharpoons F_{ij} m_j;$$

$$\boldsymbol{\mathcal{K}} : \mathbf{L} \rightleftharpoons \mathcal{K}_{ijkl} L_{lk} \text{ and } \boldsymbol{\tau} \cdot \mathbf{D} \rightleftharpoons \tau_{ik} D_{kj} .$$

The dyadic product of two side-by-side tensors yields a tensor with a rank equal to the sum of the ranks; an example is $\mathbf{sm} \rightleftharpoons s_i m_j$. Finally, time derivatives are denoted by superposed dots, e.g.,

$$\dot{\mathbf{F}} = \partial \mathbf{F} / \partial t .$$

2. Constitutive Relations for Single Crystals

The description of the rate-dependent finite-strain behavior of single crystals deforming by crystallographic slip accompanied by elastic-lattice distortion presented here follows from the work of Asaro and Needleman (1985).

2.1 Single-Crystal Kinematics

Plastic deformation is assumed to occur by simple shears along the various slip systems of the crystal. This shear is described in a bulk continuum framework and is due to dislocation movement along the slip systems or other mechanisms that produce simple shear. In addition to the plastic shearing, the lattice undergoes elastic distortion and rigid-body rotation. The motion of the single crystal can then be decomposed into a plastic part, which describes crystallographic glide, and an elastic part, which contains lattice stretching and rotation. If $\mathbf{F}$ designates the deformation gradient of the single crystal, a multiplicative decomposition of the type due to Lee (1969) is written as

$$\mathbf{F} = \mathbf{F}^* \cdot \mathbf{F}^p, \tag{1}$$

where $\mathbf{F}^p$ is due to the net motion of dislocations, and $\mathbf{F}^*$ contains the elastic distortion and rigid-body rotation of the lattice (Rice 1971; Hill and Havner 1982; Asaro 1983). The slip direction of a particular system, α, is denoted by $\mathbf{s}^{(\alpha)}$ and must lie in the slip plane with normal $\mathbf{m}^{(\alpha)}$. The orthonormal pair $\mathbf{s}^{(\alpha)}$ and $\mathbf{m}^{(\alpha)}$ convect with the lattice to become

$$\begin{aligned} \mathbf{s}^{*(\alpha)} &= \mathbf{F}^* \cdot \mathbf{s}^{(\alpha)} \\ \mathbf{m}^{*(\alpha)} &= \mathbf{m}^{(\alpha)} \cdot \mathbf{F}^{*-1} . \end{aligned} \tag{2}$$

Note that the total velocity gradient $\mathbf{L}$, can be decomposed into its elastic and plastic parts, $\mathbf{L}^*$ and $\mathbf{L}^p$, as

$$\mathbf{L} = \dot{\mathbf{F}} \cdot \mathbf{F}^{-1} = \mathbf{L}^* + \mathbf{L}^p . \tag{3}$$

The plastic part of the velocity gradient can be decomposed into its symmetric and skew symmetric parts $\mathbf{D}^p$ and $\mathbf{\Omega}^p$, respectively, as

$$\mathbf{L}^p = \mathbf{D}^p + \mathbf{\Omega}^p \,. \tag{4}$$

We incorporate equation (2) into the single-crystal kinematics by writing $\mathbf{L}^p$ in terms of the shear rates on each system. Thus,

$$\mathbf{L}^p = \sum_\alpha \mathbf{s}^{*(\alpha)} \mathbf{m}^{*(\alpha)} \dot{\gamma}^{(\alpha)}, \tag{5}$$

where α is summed over all active slip systems, and $\dot{\gamma}^{(\alpha)}$ is the rate of shearing on slip system α. For each slip system, the symmetric and antisymmetric parts of the Schmid tensor are defined as

$$\mathbf{P}^{(\alpha)} = \frac{1}{2}[\mathbf{s}^{*(\alpha)} \mathbf{m}^{*(\alpha)} + \mathbf{s}^{*(\alpha)} \mathbf{m}^{*(\alpha)}], \tag{6}$$

and

$$\mathbf{W}^{(\alpha)} = \frac{1}{2}[\mathbf{s}^{*(\alpha)} \mathbf{m}^{*(\alpha)} - \mathbf{s}^{*(\alpha)} \mathbf{m}^{*(\alpha)}], \tag{7}$$

so that

$$\mathbf{D}^p = \sum_\alpha \mathbf{P}^{(\alpha)} \dot{\gamma}^{(\alpha)}, \tag{8}$$

and

$$\mathbf{\Omega}^p = \sum_\alpha \mathbf{W}^{(\alpha)} \dot{\gamma}^{(\alpha)} \,. \tag{9}$$

The total stretch tensor $\mathbf{D}$ and the total spin $\mathbf{\Omega}$ are decomposed as $\mathbf{D} = \mathbf{D}^p + \mathbf{D}^*$ and $\mathbf{\Omega} = \mathbf{\Omega}^p + \mathbf{\Omega}^*$, where $\mathbf{D}^*$ is the elastic stretch tensor, and $\mathbf{\Omega}^*$ is the lattice spin.

2.2 Crystal Elasticity

If we denote the Kirchhoff stress as τ, the Jaumann rate of this stress, $\overset{\nabla}{\boldsymbol{\tau}}$, on axes that spin with the material is

$$\overset{\nabla}{\boldsymbol{\tau}} = \dot{\tau} - \mathbf{\Omega} \cdot \tau + \tau \cdot \mathbf{\Omega} \,. \tag{10}$$

We can also write the Jaumann rate of Kirchoff stress , $\overset{\nabla}{\boldsymbol{\tau}}^*$, formed on axes that spin with the lattice as

$$\overset{\nabla}{\boldsymbol{\tau}}^* = \dot{\tau} - \mathbf{\Omega}^* \cdot \tau + \tau \cdot \mathbf{\Omega}^* \,. \tag{11}$$

As shown by Asaro and Needleman (1985), for a material characterized by an elastic-strain energy function (elastic moduli, $\mathcal{L}$), $\overset{\nabla}{\boldsymbol{\tau}}^*$ is given by

$$\overset{\nabla}{\boldsymbol{\tau}}^* = \mathcal{L} : \mathbf{D}^* + \mathbf{D}^* \cdot \tau + \tau \cdot \mathbf{D}^* \approx \mathcal{L} : \mathbf{D}^* \,. \tag{12}$$

This approximation is due to the assumption that stresses are small compared to elastic moduli. We incorporate equations (9) and (10) into equation (11) to get

$$\overset{\nabla}{\boldsymbol{\tau}}^* = \overset{\nabla}{\boldsymbol{\tau}} + \sum_\alpha \{\mathbf{W}^{(\alpha)} \cdot \tau - \tau \cdot \mathbf{W}^{(\alpha)}\} \dot{\gamma}^{(\alpha)} \,. \tag{13}$$

Equation (13) is now substituted into equation (12). The resulting constitutive law is written as

$$\overset{\nabla}{\boldsymbol{\tau}} = \boldsymbol{\mathcal{L}} : \mathbf{D} - \sum_{\alpha} \{ \boldsymbol{\mathcal{L}} : \mathbf{P}^{(\alpha)} + \mathbf{W}^{(\alpha)} \cdot \boldsymbol{\tau} - \boldsymbol{\tau} \cdot \mathbf{W}^{(\alpha)} \} \dot{\gamma}^{(\alpha)} \, . \tag{14}$$

This expression is often written in more concise form as

$$\overset{\nabla}{\boldsymbol{\tau}} = \boldsymbol{\mathcal{L}} : \mathbf{D} - \sum_{\alpha} \mathbf{R}^{(\alpha)} \dot{\gamma}^{(\alpha)} \, . \tag{15}$$

2.3 Slip Constitutive Model

To capture the dynamic behavior of Ta at high strain rates, the slip constitutive law at time t will depend on the current stress state and system resistance to glide, τ and $g^{(\alpha)}$, respectively, as well as the current temperature, T, in the deforming crystal. Generally, the shear rate $\dot{\gamma}^{(\alpha)}$ of the system α can be specified by a function with the form

$$\dot{\gamma}^{(\alpha)}(t) = \dot{\tilde{\gamma}}^{(\alpha)}(\tau, g^{(\alpha)}, \mathrm{T}) \, . \tag{16}$$

The specific form that we will examine is a modification of a widely used power law due to Lee et al. (1997) that relates these shear rates to their conjugate measure of stresses (i.e., resolved shear stresses) $\tau^{(\alpha)}$, viz.,

$$\tau^{(\alpha)} = g^{(\alpha)} \left(\frac{\dot{\gamma}^{(\alpha)}}{\dot{\gamma}_0} \right)^m sgn(\dot{\gamma}^{(\alpha)}) \exp(-\lambda \Delta T), \tag{17}$$

where $\dot{\gamma}_0$ is a reference shear rate assumed the same for all slip systems, m is the strain-rate sensitivity coefficient, λ is the thermal softening coefficient, and ΔT is the temperature increase from a reference temperature $(T - T_{ref})$. The reference temperature for this work is taken as ambient room temperature. Initially, each $g^{(\alpha)}$ is taken to be a constant that can be different from one slip system to another, and the rate of increase of these resistances is specified by the following hardening law:

$$\dot{g}^{(\alpha)} = \sum_{\beta} h^{\alpha\beta} \left| \dot{\gamma}^{(\beta)} \right|, \tag{18}$$

and

$$h^{\alpha\beta} = q^{\alpha\beta} h^{\beta} \ \ (\text{no sum on } \beta), \tag{19}$$

where $q^{\alpha\beta}$ is a matrix fully populated by ones. The single-slip hardening rate, h^{β}, will be given the saturation form proposed by Kalidindi, Bonchorst, and Anand (1992);

$$h^{\beta} = h_0 \left(1 - \frac{g^{\alpha}}{g_s^{\alpha}} \right)^a , \tag{20}$$

where g_s^α is the saturation resistance to slip. The expression for the dissipation of mechanical work into heat during high-strain-rate deformation is given as

$$\Delta T = \int_0^t \frac{\chi}{\rho C_\rho} \sum_\alpha \tau^\alpha \dot{\gamma}^\beta dt, \tag{21}$$

where $0 \leq \chi \leq 1$ represents the fraction of plastic work that is converted to heat, ρ is the density, and C_ρ is the heat capacity.

2.4 Determination of the Slip Planes

In this work, high rate deformation in Ta is assumed to occur by pencil glide along the $< 111 >$ crystallographic directions. The slip planes will not be restricted to any specific set of crystallographic planes, but will be allowed to occur on any plane that maximizes the resolved shear stress for a particular slip direction. The following method has been proposed by Becker (1995) for the determination of the plane that maximizes the resolved shear stress. For a particular slip system, α, the resolved shear stress τ^α is given as a function of the slip geometry and the applied stress

$$\tau^{(\alpha)} = \mathbf{m}^{*(\alpha)} \cdot \boldsymbol{\tau} \cdot \mathbf{s}^{*(\alpha)} = \mathbf{m}^{*(\alpha)} \cdot \mathbf{t}^{*(\alpha)} . \tag{22}$$

The vector $\mathbf{t}^{*(\alpha)}$ represents the traction normal to the slip direction in the updated configuration.

Note that τ^α is maximum when $\mathbf{m}^{*(\alpha)}$ lies in the direction of $\mathbf{t}^{*(\alpha)}$. The slip-plane normal, therefore, is calculated by removing the component of $\mathbf{t}^{*(\alpha)}$ in the direction of $\mathbf{s}^{*(\alpha)}$ (to assure orthogonality between $\mathbf{s}^{*(\alpha)}$ and $\mathbf{m}^{*(\alpha)}$). Normalization of the the slip-plane normal then yields

$$\mathbf{m}^{*(\alpha)} = \frac{\mathbf{t}^{*(\alpha)} - (\mathbf{s}^{*(\alpha)} \cdot \mathbf{t}^{*(\alpha)})\mathbf{s}^{*(\alpha)}}{|\mathbf{t}^{*(\alpha)} - (\mathbf{s}^{*(\alpha)} \cdot \mathbf{t}^{*(\alpha)})\mathbf{s}^{*(\alpha)}|} . \tag{23}$$

The plane normal is computed for each of the four slip directions. Thus, only four slip systems are selected instead of 12, 24, or 48, as in the case of restricted glide; this results in an important computational time reduction.

2.5 Numerical Implementation.

During the computations, care must be taken in order to estimate the actual slip rates over a given time increment. In order to obtain a conditionally stable, explicit integration of the stress rate across a time step, the tangent modulus method of Peirce, Asaro, and Needleman (1983) is employed. The following is a modification of their method in order to accommodate the temperature-dependent slip-rate constitutive model. By expanding equation (16) in a Taylor series about the current time t, we can estimate the increment in slip across the current time step.

$$\dot{\gamma}^\alpha(t + \Delta t) = \dot{\gamma}^\alpha(t) + \frac{\partial \dot{\gamma}^\alpha(t)}{\partial g^\alpha} \Delta g^\alpha +$$

$$\frac{\partial \dot{\gamma}^\alpha(t)}{\partial \tau^\alpha}\Delta\tau^\alpha + \frac{\partial \dot{\gamma}^\alpha(t)}{\partial \mathrm{T}}\Delta\mathrm{T}\,. \tag{24}$$

We insert equation (17) into equation (24) to yield

$$\dot{\gamma}^\alpha(t+\Delta t) = \left[1 + \tfrac{1}{m}\left(\tfrac{\Delta\tau^\alpha}{\tau^\alpha} + \tfrac{\Delta g^\alpha}{g^\alpha} + \lambda\Delta\mathrm{T}\right)\right]\dot{\gamma}^\alpha(t)\,. \tag{25}$$

The increment of slip across the time step, defined by

$$\Delta\gamma^\alpha = \gamma^\alpha(t+\Delta t) - \gamma^\alpha(t), \tag{26}$$

is approximated by Pierce, Asaro, and Needleman (1983) as a linear interpolation across the time step

$$\Delta\gamma^\alpha = \left[(1-\theta)\dot{\gamma}^\alpha(t) + \theta\dot{\gamma}^\alpha(t+\Delta t)\right]\Delta t, \tag{27}$$

where θ is an interpolation parameter taken here as 0.5. Substitution of equation (25) into the previous equation, equation (27), yields

$$\Delta\gamma^\alpha = \left[\dot{\gamma}^\alpha(t) + \frac{\theta\dot{\gamma}^\alpha(t)}{m}\left(\frac{\Delta\tau^\alpha}{\tau^\alpha} + \frac{\Delta g^\alpha}{g^\alpha} + \lambda\Delta\mathrm{T}\right)\right]\Delta t\,. \tag{28}$$

Using $\Delta\tau = \dot{\tau}\Delta t$, $\Delta g = \dot{g}\Delta t$ and equation (21) for ΔT in equations (28) and (27) we get

$$\Delta\gamma^\alpha = \dot{\gamma}^\alpha(t)\Delta t + \frac{\theta\Delta t\dot{\gamma}^\alpha(t)}{m\tau^\alpha}\left[\mathbf{R}^\alpha : \mathbf{D} - \sum_\beta\left(\mathbf{R}^\alpha : \mathbf{P}^\beta + \frac{\tau^\alpha}{g^\alpha}h_{\alpha\beta} - \frac{\lambda\chi}{\rho\mathrm{C}_v}\tau^\alpha\tau^\beta\right)\dot{\gamma}^\beta(t)\right]\,. \tag{29}$$

This estimate for the increment of slip across the time step is now simplified and made consistent with the original Pierce, Asaro, and Needleman (1983) notation. By expressing

$$\mathbf{Q}^\alpha = \left(\frac{\theta\Delta t\dot{\gamma}^\alpha(t)}{m\tau^\alpha}\right)\mathbf{R}^\alpha \tag{30}$$

and

$$N_{\alpha\beta} = \delta_{\alpha\beta} + \left(\frac{\theta\Delta t\dot{\gamma}^\alpha(t)}{m\tau^\alpha}\right) \times \left[\frac{\mathbf{R}^\alpha : \mathbf{P}^\beta}{\tau^\alpha} + \frac{h^{\alpha\beta}}{g^\alpha} - \frac{\lambda\chi\tau^\beta}{\rho\mathrm{C}_v}\right]\,. \tag{31}$$

We can now substitute equation (29) into equation (15) for a stable estimate of the stress rates across the time step;

$$\overset{\nabla}{\boldsymbol{\tau}} = \mathbf{C} : \mathbf{D} - \sum_\alpha \mathbf{R}^\alpha \dot{f}^\alpha, \tag{32}$$

with

$$\begin{aligned} \mathbf{C} &= \boldsymbol{\mathcal{L}} - \sum_\alpha \mathbf{R}^\alpha\mathbf{F}^\alpha, \\ \mathbf{F}^\alpha &= \sum_\beta M_{\alpha\beta}\mathbf{Q}^\beta, \\ \dot{f}^\alpha &= \sum_\beta M_{\alpha\beta}\dot{\gamma}^\alpha(t)\,. \end{aligned} \tag{33}$$

The matrix M is the inverse of N (guaranteed invertible for sufficiently small time steps) (Pierce, Asaro, and Needleman 1983).

2.6 Polycrystal Averaging

The modified Taylor polycrystal averaging scheme (e.g., Asaro and Needleman 1985) is incorporated in order to (1) localize the macroscopic deformation to the local grains and (2) average the resulting stresses from the local grains to the associated macroscopic aggregate stresses. The model assumes that deformation within a grain is uniform and that each grain undergoes the same deformation as the entire aggregate. Therefore, the local velocity gradient, $\mathbf{L}$, is identical to the macroscopic velocity gradient, $\bar{\mathbf{L}}$. In this way, deformation compatibility between the grains and macroscopic deformation is maintained. After localization of the applied $\bar{\mathbf{L}}$ to $\mathbf{L}$, the local Cauchy stresses, $\mathbf{S}$, are then calculated and volume-averaged to achieve the macroscopic stress, $\bar{\mathbf{S}}$. Since the calculations assume that all the grains occupy an equal volume within the polycrystal,

$$\bar{\mathbf{S}} = \frac{1}{K}\sum_{g=1}^{K}\mathbf{S}^{(g)}, \tag{34}$$

where K is the number of grains in the aggregate.

3. Results and Discussion

Lee et al. (1997) compressed samples of pure Ta at strain rates ranging from 0.001/s to 30,000/s and temperatures ranging from 25°C to 525°C. The previously described model for pencil-glide has been calibrated to their room-temperature data at a strain rate of 3,000/s via the following procedure. The elastic constants were taken from Gray and Vecchio (1995) as $C_{11} = 260.9$ GPa, $C_{12} = 15.74$ GPa, and $C_{44} = 81.8$ Gpa. The thermal-softening parameter, λ, was set to $0.00153K^{-1}$ to reflect the thermal softening observed from Lee et al. (1997) between their quasi-static room-temperature data and data taken at 325°C. The portion of mechanical work converted to heat, χ, was assumed to be 0.9. The initial resistance to slip, g_0^α was estimated at 154 MPa and taken to be equal on all slip systems, while the reference shear rate was taken to be $\dot{\gamma}_0 = 1000/\text{s}$. The strain-rate hardening exponent was taken as $m = 0.084$ accounting for the strain-rate sensitivity between their quasi-static and 3,000/s data at an offset strain of 0.05. Since the strain-hardening behavior at large strains (> 0.2) is quite different between these two sets of data, it is not expected that a single set of parameters will model this entire data set for the current model. The remaining set of material parameters were fit using the minimization routine "e04upf" in the NAG library in order to minimize

$$\Phi(\mathbf{x}) = \frac{1}{2}\mathbf{f}(\mathbf{x})\cdot\mathbf{f}(\mathbf{x}), \tag{35}$$

where

$$\mathbf{f}(\mathbf{x}) = \frac{1}{n}\sum_{1}^{n}\frac{S_{22}^{experiment}(\epsilon_{22}) - S_{22}^{calculation}(\epsilon_{22})}{S_{22}^{experiment}(\epsilon_{22})} \tag{36}$$

over n data points.

The components of $\mathbf{x}$ are taken as the strain-hardening constants for the slip constitutive law; h_0, g_s^α, and a. $S_{22}(\epsilon_{22})$ is the component of stress along the compression direction for the sample. Figure 1 shows the resulting fit for uniaxial compression at $3,000/s$. The strain-hardening constants are given as $h_0 = 2498.6$ MPa, $g_s^\alpha = 231.6$ MPa, and $a = 1.08$.

The deformation texture predicted from this calibrated model is compared to equivalent textures resulting from restricted-glide on the $< 111 > \{110\}$ and $< 111 > \{121\}$ systems in Figure 2. After a true strain of 0.70, both models compare well to the experimentally measured textures found in Lee et al. (1997) and are nearly indistinguishable from one another. It is important to note here that the restricted glide calculation over 24 slip systems required almost 20 times more computational effort than the pencil-glide calculation over four slip systems; yet, both produce macroscopically equivalent grain distributions.

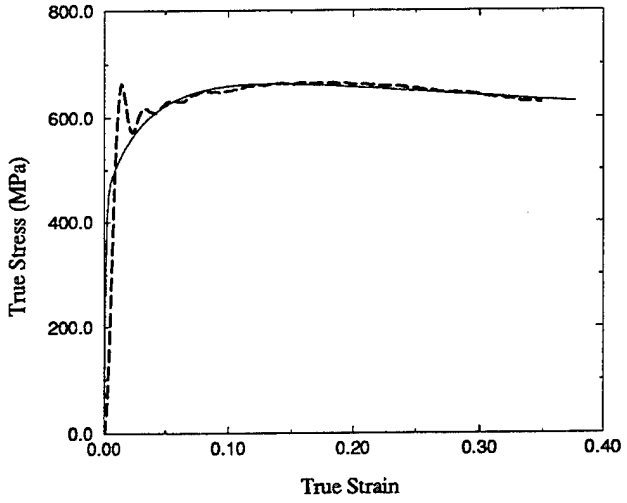

Figure 1. Pencil-glide model (solid line) calibrated to the stress-strain data of Lee et al. (1997) (dashed line).

In order to understand how these equivalent textures evolve, a single grain was simulated to undergo uniaxial compression along the crystallographic $< 100 >$, $< 110 >$ and $< 111 >$ directions. Table 1 summarizes the calculated slip-plane normals at the onset of plastic straining (a Mises effective stain of ≈ 0.005). It is interesting to note that the slip-plane normals for compression along the $< 100 >$ and $< 110 >$ directions are $\{110\}$ and $\{121\}$, consistent with those observed in bcc materials. During compression along the $< 111 >$, the calculated normals are very close to the $\{123\}$ planes, which are also observed slip planes in bcc materials. Since the restricted-glide model incorporated the $< 111 > \{110\}$ and $< 111 > \{121\}$ systems explicitly, calculated grain rotations were almost identical for the two models. Perhaps more importantly, however, is the fact that the pencil glide model seeks to maximize the resolved shear stress along the slip direction based on the overall stress state in the grain. The stress response in the grain is due to the incorporation of the single-crystal

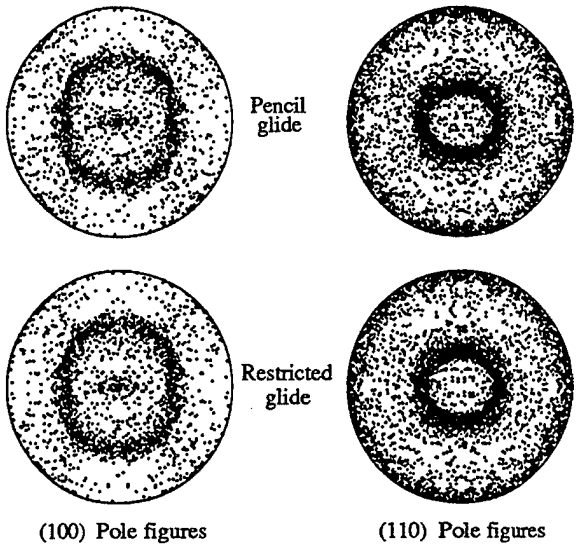

Figure 2. Calculated pole figures for uniaxial compression of 300 initially random-oriented grains using (a) the pencil-glide model with four $< 111 >$ directions and (b) a restricted-glide model with 24 $< 111 > \{110\}$ and $< 111 > \{121\}$ systems.

elasticity and is therefore perhaps more physically meaningful than restricting slip to only the "observed" slip systems.

In closing, it should be noted that a temperature-dependent elastic-viscoplastic model for pencil glide has been introduced and shown capable of representing the mechanical behavior and texture evolution in pure polycrystalline Ta. This new model calculates slip planes so as to maximize the resolved shear stress in the slip direction via the stresses due to elastic-lattice distortion and therefore provides a physically based description of the active deformation mechanisms.

Compression Axis	Slip Direction	Plane Normal
1 0 0	1 1 1	1.00 -2.00 1.00
	-1 1 1	-1.00 -2.00 1.00
	-1 -1 1	-1.00 2.00 1.00
	1 -1 1	1.00 2.00 1.00
1 1 0	1 1 1	1.00 -1.00 2.00
	-1 1 1	-1.00 -1.00 0.00
	-1 -1 1	1.00 1.00 2.00
	1 -1 1	1.00 1.00 0.00
1 1 1	1 1 1	-2.00 1.00 1.00
	-1 1 1	-2.00 -1.00 -1.00
	-1 -1 1	1.78 1.00 2.78
	1 -1 1	-1.78 -2.78 -1.00

Table 1. Calculated slip-plane normals as a function of compression direction for a single crystal under uniaxial compression.

4. References

1. Asaro, R. J. "Crystal Plasticity." *Journal of Applied Mechanics*, vol. 5, p. 921, 1983.
2. Asaro, R. J., and A. Needleman, "Texture Development and Strain Hardening in Rate Dependent Polycrystals." *Acta Metallurgica et materialia*, vol. 33, p. 923, 1985.
3. Backofen, W. A., *Deformation Processing*, Addison-Wesley, Reading, Massachusetts, 1972.
4. Becker, R. C., "Pencil Glide Formulation for Polycrystal Modelling." *Scripta Metallurgica et Materialia*, vol. 32, p. 2051, 1995.
5. Clark, J. B., R. K. Garrett Jr., R. A. Jungling, R. A. Vandermeer and C. L. Vold,"Effect of Processing Variables on Texture and Texture Gradients in Tantalum." *Metallurgical and Materials Transactions A.*, p. 2039, 1991.
6. Gray, G. T. and K. S. Vecchio, "Influence of Peak Pressure and Temperature on the Sructure/Property Response of Shock-Loaded Ta and Ta-10W." *Metallurgical and Materials Transactions A.*, vol. 26, p. 2525, 1995.
7. Hill, R. and K. S. Havner, "Perspectives in the mechanics of elastoplastic crystals." *Journal of the Mechanics and Physics of Solids*, vol. 30, p. 5, 1982.
8. Kalidindi, S. R., C. A. Bronkhorst and L. Anand, "Crystallographic Texture Evolution in Bulk Deformation Processing of FCC Metals," *Journal of the Mechanics and Physics of Solids*, vol. 40, 537, 1992.
9. Lankford, W. T., S. C. Snyder and J. A. Bauscher, *Society of Mining Engineers, AIME transactions*, vol. 42, p. 1197, 1950.
10. Lee, E. H., "Elastic-Plastic Deformation at Finite Strains." *Journal of Applied Mechanics*, vol. 36, p. 1, 1969.
11. Lee, B. J., K. S. Vecchio, S. Ahzi and S. E. Schoenfeld, "Modeling Mechanical Behavior of Tantalum." *Metallurgical and Materials Transactions A.*, vol. 28A, p. 113, 1997.
12. Pierce, D., R. J. Asaro and A. Needleman, "Material Rate Dependence and Localized Deformation in Crystalline Solids." *Acta Metallurgica et materialia*, vol. 31, p. 1951, 1983.
13. Rice, J. R., "Inelastic Constitutive Relations for Solids: An Internal-Variable Theory and its Application to Metal Plasticity," *Journal of the Mechanics and Physics of Solids*, vol. 19, p. 433, 1971.

INTENTIONALLY LEFT BLANK

NO. OF COPIES	ORGANIZATION
2	DEFENSE TECHNICAL INFORMATION CENTER DTIC DDA 8725 JOHN J KINGMAN RD STE 0944 FT BELVOIR VA 22060-6218
1	HQDA DAMO FDQ DENNIS SCHMIDT 400 ARMY PENTAGON WASHINGTON DC 20310-0460
1	CECOM SP & TRRSTRL COMMCTN DIV AMSEL RD ST MC M H SOICHER FT MONMOUTH NJ 07703-5203
1	PRIN DPTY FOR TCHNLGY HQ US ARMY MATCOM AMCDCG T M FISETTE 5001 EISENHOWER AVE ALEXANDRIA VA 22333-0001
1	PRIN DPTY FOR ACQUSTN HQS US ARMY MATCOM AMCDCG A D ADAMS 5001 EISENHOWER AVE ALEXANDRIA VA 22333-0001
1	DPTY CG FOR RDE HQS US ARMY MATCOM AMCRD BG BEAUCHAMP 5001 EISENHOWER AVE ALEXANDRIA VA 22333-0001
1	DPTY ASSIST SCY FOR R&T SARD TT T KILLION THE PENTAGON WASHINGTON DC 20310-0103
1	OSD OUSD(A&T)/ODDDR&E(R) J LUPO THE PENTAGON WASHINGTON DC 20301-7100

NO. OF COPIES	ORGANIZATION
1	INST FOR ADVNCD TCHNLGY THE UNIV OF TEXAS AT AUSTIN PO BOX 202797 AUSTIN TX 78720-2797
1	USAASA MOAS AI W PARRON 9325 GUNSTON RD STE N319 FT BELVOIR VA 22060-5582
1	CECOM PM GPS COL S YOUNG FT MONMOUTH NJ 07703
1	GPS JOINT PROG OFC DIR COL J CLAY 2435 VELA WAY STE 1613 LOS ANGELES AFB CA 90245-5500
1	ELECTRONIC SYS DIV DIR CECOM RDEC J NIEMELA FT MONMOUTH NJ 07703
3	DARPA L STOTTS J PENNELLA B KASPAR 3701 N FAIRFAX DR ARLINGTON VA 22203-1714
1	SPCL ASST TO WING CMNDR 50SW/CCX CAPT P H BERNSTEIN 300 O'MALLEY AVE STE 20 FALCON AFB CO 80912-3020
1	USAF SMC/CED DMA/JPO M ISON 2435 VELA WAY STE 1613 LOS ANGELES AFB CA 90245-5500
1	US MILITARY ACADEMY MATH SCI CTR OF EXCELLENCE DEPT OF MATHEMATICAL SCI MDN A MAJ DON ENGEN THAYER HALL WEST POINT NY 10996-1786

NO. OF
COPIES ORGANIZATION

1 DIRECTOR
US ARMY RESEARCH LAB
AMSRL CS AL TP
2800 POWDER MILL RD
ADELPHI MD 20783-1145

1 DIRECTOR
US ARMY RESEARCH LAB
AMSRL CS AL TA
2800 POWDER MILL RD
ADELPHI MD 20783-1145

3 DIRECTOR
US ARMY RESEARCH LAB
AMSRL CI LL
2800 POWDER MILL RD
ADELPHI MD 20783-1145

ABERDEEN PROVING GROUND

4 DIR USARL
AMSRL CI LP (305)

NO. OF COPIES ORGANIZATION

2 DIRECTOR
LLNL
L-170 D LASSILA
L-355 A SCHWARTZ
P O BOX 808
LIVERMORE CA 94550

1 NSWC
INDIAN HEAD DIVISION
R K GARRET JR
BLDG 841 RM 20
101 STRAUSS AVE
INDIAN HEAD MD 20640

1 NSWC
CARDEROCK DIVISION
JOHN MCKIRGAN
9500 MACARTHUR BLVD
WEST BETHESDA MD 20817-5700

1 COMMANDER
US ARMY ARDEC
ATTN AMSTA AR FSA E
E BAKER
PICATINNY ARSENAL NJ
07806-5000

ABERDEEN PROVING GROUND

68 DIR, USARL
AMSRL-WM-T, W MORRISON
AMSRL-WM-TD,
A DIETRICH
T FARRAND
K FRANK
S SCHOENFELD (12 CP)
A GUPTA
M RAFTENBERG
M SCHEIDLER
S SEGLETES
J WALTER
T WRIGHT
AMSRL-WM-TC,
W DE ROSSET
K KIMSEY
M LAMPSON
L MAGNESS
D SCHEFFLER
G SILSBY

NO. OF COPIES ORGANIZATION

AMSRL-WM-TC (continued),
R SUMMERS
W WALTERS
AMSRL-WM-TA,
S BILYK
W BRUCHEY
G BULMASH
M BURKINS
J DEHN
G FILBEY
W GILLICH
W GOOCH
D HACKBARTH
T HAVEL
E HORWATH
Y HUANG
H MEYER
E RAPACKI
J RUNYEON
N RUPERT
M ZOLTOSKI
AMSRL-WM-WD, A NIILER
AMSRL-WM-MF,
S CHOU
D DANDEKAR
R RAJENDRAN
T WEERASOORIYA
D GROVE
AMSRL-WM-M,
D VIECHNICKI
J MCCAULY
G HAGNAUER
AMSRL-WM-ME,
M WELLS
R ADLER
M STAKER
AMSRL-WM-MC,
M CHEN
G GILDE
P HUANG
T HYNES
J SWAB
J WELLS
J CASALVIA
C HUBBARD
M COLE

INTENTIONALLY LEFT BLANK

REPORT DOCUMENTATION PAGE

Form Approved
OMB No. 0704-0188

1. AGENCY USE ONLY *(Leave blank)*	2. REPORT DATE	3. REPORT TYPE AND DATES COVERED
	October 1997	Final, April 195 - September 1995

4. TITLE AND SUBTITLE

Modeling Dynamic Behavior and Texture Evolution in Pure Tantalum (Ta)

5. FUNDING NUMBERS

61102AH43

6. AUTHOR(S)

S. E. Schoenfeld, S. Ahzi.,* and K. S. Vecchio**

7. PERFORMING ORGANIZATION NAME(S) AND ADDRESS(ES)

U.S. Army Research Laboratory
ATTN: AMSRL-WM-TD
Aberdeen Proving Ground, MD 21005-5066

8. PERFORMING ORGANIZATION REPORT NUMBER

ARL-TR-1530

9. SPONSORING/MONITORING AGENCY NAMES(S) AND ADDRESS(ES)

10.SPONSORING/MONITORING AGENCY REPORT NUMBER

11. SUPPLEMENTARY NOTES

*Department of Mechanical Engineering, Clemson University
**Department of Applied Mechanics and Engineering Science, University of California, San Diego

12a. DISTRIBUTION/AVAILABILITY STATEMENT

Approved for public release; distribution is unlimited.

12b. DISTRIBUTION CODE

13. ABSTRACT *(Maximum 200 words)*

In order to model high-strain-rate deformation and texture evolution in commercially pure tantalum (Ta), a description for the thermal-elastic-viscoplastic behavior of Ta single crystals is considered along with an associated polycrystal averaging scheme. The description incorporates a temperature-dependent model for pencil glide on the planes of maximum-resolved shear stress. Calculated stress-strain data and texture evolution for this model are compared to those of a restricted-glide model and to experimental data.

14. SUBJECT TERMS

tantalum, polycrystal modeling

15. NUMBER OF PAGES

21

16. PRICE CODE

17. SECURITY CLASSIFICATION OF REPORT	18. SECURITY CLASSIFICATION OF THIS PAGE	19. SECURITY CLASSIFICATION OF ABSTRACT	20. LIMITATION OF ABSTRACT
UNCLASSIFIED	UNCLASSIFIED	UNCLASSIFIED	UL

NSN 7540-01-280-5500

Standard Form 298 (Rev. 2-89)
Prescribed by ANSI Std. 239-18 298-102

INTENTIONALLY LEFT BLANK

USER EVALUATION SHEET/CHANGE OF ADDRESS

This Laboratory undertakes a continuing effort to improve the quality of the reports it publishes. Your comments/answers to the items/questions below will aid us in our efforts.

1. ARL Report Number/Author ARL-TR-1530 (Schoenfeld) Date of Report October 1997

2. Date Report Received _____

3. Does this report satisfy a need? (Comment on purpose, related project, or other area of interest for which the report will be used.) _____

4. Specifically, how is the report being used? (Information source, design data, procedure, source of ideas, etc.) _____

5. Has the information in this report led to any quantitative savings as far as man-hours or dollars saved, operating costs avoided, or efficiencies achieved, etc? If so, please elaborate. _____

6. General Comments. What do you think should be changed to improve future reports? (Indicate changes to organization, technical content, format, etc.) _____

CURRENT ADDRESS

Organization

Name E-mail Name

Street or P.O. Box No.

City, State, Zip Code

7. If indicating a Change of Address or Address Correction, please provide the Current or Correct address above and the Old or Incorrect address below.

OLD ADDRESS

Organization

Name

Street or P.O. Box No.

City, State, Zip Code

(Remove this sheet, fold as indicated, tape closed, and mail.)

(DO NOT STAPLE)

DEPARTMENT OF THE ARMY

OFFICIAL BUSINESS

NO POSTAGE
NECESSARY
IF MAILED
IN THE
UNITED STATES

BUSINESS REPLY MAIL
FIRST CLASS PERMIT NO 0001,APG,MD

POSTAGE WILL BE PAID BY ADDRESSEE

DIRECTOR
US ARMY RESEARCH LABORATORY
ATTN AMSRL WM TD
ABERDEEN PROVING GROUND MD 21005-5066